ACTA STEREOL 1995; 14/2: 215-222
ORIGINAL SCIENTIFIC PAPER

CONTRIBUTION OF IMAGE ANALYSIS TO SOLID STATE SINTERING OF WC-CO

Sophie Roure, Jean-Michel Missiaen

Laboratoire de Thermodynamique et Physico-Chimie Métallurgiques, ENSEEG domaine universitaire BP 75, 38402 St Martin d'Hères Cedex, France
e-mail: sroure@ltpcm.grenet.fr Fax: +(33) 76 82 67 44

ABSTRACT

Solid-state sintering of the WC-Co system has been studied by image analysis. Automatic phase segmentation and measurements were possible through the combination of optimized specimen preparation, high spatial resolution in S.E.M., and image processing in a software oriented image analyzer. Three phases could thus be extracted from the microstructure, the carbide phase (WC), the binder phase (Co) and the porous phase, in order to evaluate for each one classical stereological parameters like volume fraction or specific contact surfaces. As well, using mathematical morphology through measurements of chord length distribution and covariance, some major features of solid phase sintering of the WC-Co system could be characterized: quantitative and morphological evolution of porosity with sintering temperature, wetting of the carbide grains by the binder, rearrangement and shape accomodation processes.

Key words: cemented carbide, linear granulometry, rearrangement, solid state sintering, specific surface area.

INTRODUCTION

In manufacturing, cemented carbides are produced by liquid phase sintering, a process which has been thoroughly investigated both experimentally and theoretically. The classical analysis (Kingery, 1959) assumes that no structural change occurs before the formation of liquid and that densification takes place rapidly under capillary forces as soon as the binder phase melts. However, dilatometry studies (Åkesson, 1979; Haglund et al., 1994) have revealed that an important part of densification during sintering of WC-Co takes place during the heating, before the liquid forms (below T≈1300°C). Solid state sintering should therefore be considered as a major step in the densification process of WC-Co. This study is a part of a research program which attempts to determine the influence of compaction on sintering of WC-Co alloys. In this context, it will aim at characterizing the microstructural evolution from the compacted state to the sintered state by emphasizing the role of solid state sintering.

MATERIAL AND EXPERIMENTAL PROCEDURE

Specimen preparation

Compact specimens of green density equal to 0.55 were obtained by uniaxial cold pressing of a WC-Co powder mixture with a carbide grain size in the range of 0.5-3μm and cobalt content of 8.5 weight % (14.2 vol.%). Sintering was performed in a dilatometer (SETARAM TMA92) in vacuum. The heating rate was 40 °C/min up to the isothermal temperature (T_s) which was held for three hours. Four temperatures have been chosen for T_s: 1000 °C, 1100 °C, 1200 °C, 1250 °C. After sintering, samples were cut into halves, infiltrated under vacuum with epoxy resin and polished. No etching was realized on specimens.

Image acquisition

Microstructures were examined by Scanning Electron Microscopy (JEOL 6400) using back-scattered images to get atomic number contrast and with a rather low accelerating voltage (10kV) to limit the penetration depth of the electrons. SEM adjustments were optimized to get the best quality of image . 15 images per sample were taken at an appropriate contrast and brightness to obtain a white WC, a grey cobalt and a black porosity. Two magnifications (M) were selected: M=6000 for microstructural characterization at the grain scale, M=1200 for porosity distribution at a larger scale.

Image analysis

An automatic image analysis system Tracor Northern 8502 was used for the measurements. The first step was to extract the three phases, the WC phase, the cobalt phase and the porosity, from the digital image. Automatic thresholding based on the maximization of interclass variance (Otsu's algorithm, 1979) was performed to obtain three preliminary binary images. Due to unavoidable superposition of grey levels between the phases in the digital image, morphological filter-based treatment should be used to get the proper binary images. Stereological parameters, like the volume fraction (Vv) and the specific surface area (Sv) were measured for each phase. Concerning the latter, the parameter Sv/Vv was preferentially employed to compare the results for one phase at various temperatures, as it is independent from the volume fraction of the phase. Covariance measurements were performed on images at 1200x magnification. Chord length distributions were also obtained. As the volume fraction of each phase is not constant with T_s due to the densification of the system, it was often more convenient for relevant comparisons to replace the density distribution function f(l) or the length-weighted density g(l) by $f(l)xN_L(X)$ or $g(l)xL_L(X)$ as the y-Axis of the granulometric curves , with $N_L(X)$ being the number of intercepts of the X phase per unit length and $L_L(X)$ the length fraction of X. Equivalent expressions are respectively dN_L/dl, the derivative of N_L by the chord length or dL_L/dl and these were the ones used in the present graphs. All the results were obtained by averaging measurements performed on the fifteen fields per sample. The field size corresponds to the whole acquired image, namely 14.8μm x 14.8μm for images at 6000x magnification (see Fig.5) and 74μm x 74μm for those at 1200x magnification (Fig.1).

RESULTS AND DISCUSSION

Porosity phase

Fig.1 illustrates the porosity evolution with the sintering temperature (T_S). Besides clear densification, it shows that small pores tend to disappear with Ts whereas the size of bigger pores seems to increase up to 1200 °C. The evolution of the porosity volume fraction with T_S

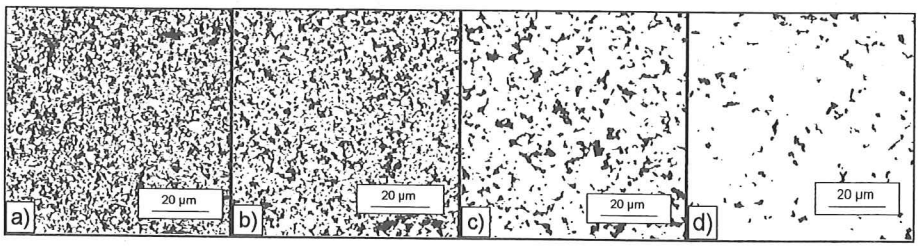

Fig.1. Binary images of the porosity (M=1200) at different temperatures: a) 1000 °C b) 1100 °C c) 1200 °C d) 1250 °C.

in Fig.2 confirms that major densification occurs in the solid state; at 1250 °C, the relative density of the sample reaches 0.9 meaning that more than 70% of the shrinkage that leads to total densification has been realized. Fig.2 also shows that Sv/Vv decreases with T_S up to

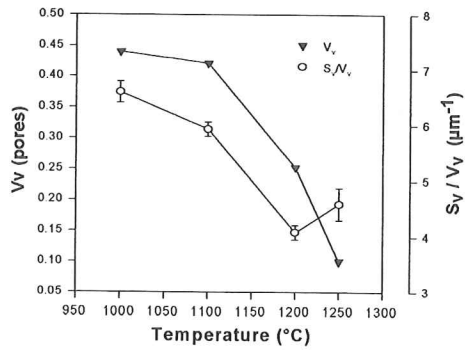

Fig.2. Evolution of Vv and Sv/Vv with the sintering temperature for the porosity phase.

1200 °C, which indicates that the porosity structure coarsens in the first stages of sintering.In order to fully characterize this evolution, chord length distribution appears as essential. For the sake of clarity, two graphs are presented in Fig.3: up to 1200 °C (a) and above 1200 °C (b).

It is seen in Fig.3a that coarsening of the pore structure results both from disappearance of small pores ($l < 2$ μm) and coarsening of large pores ($l \approx 3$-5 μm). Above 1200 °C, Fig.3b indicates that a global shrinkage of the remaining porosity takes place. Covariance of the porosity phase at 1250 °C (Fig.4) shows that the structure is correlated up to 20 μm, which is, in the light of the other results, proof that the system moves to a structure made up of dense regions and of what could be called interagglomerate porosity. This structure may result from a rearrangement of particles in the very first stages of densification which leads to the formation of agglomerates with poor porosity associated with rather large porosity in the interagglomerate space. Further, densification will proceed at first inside the agglomerates where the interparticle distance is very small and then on a larger scale leading to the shrinkage of the so-called interagglomerate porosity. At this point, a study of the binder phase is necessary to understand the driving forces involved in this process.

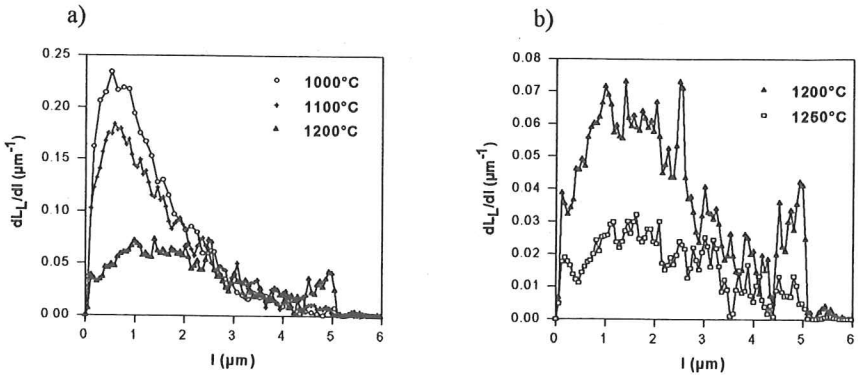

Fig.3. Granulometry of pores (length-weighted) as a function of the sintering temperature.

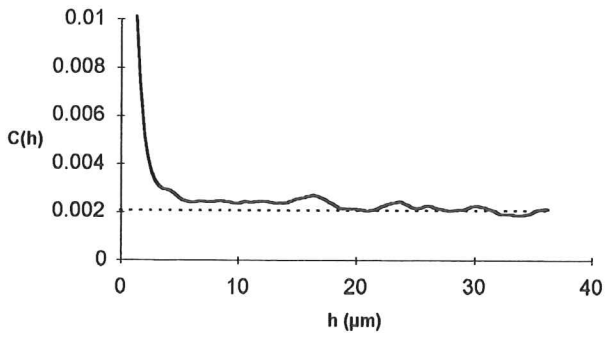

Fig.4. Covariance of the porosity phase measured from the binary image on Fig.1d).

Binder phase

Fig. 5 illustrates the microstructure evolution with the sintering temperature T_S. It can be seen that cobalt, present in the compact sample as individual grains in the range of 1-4 μm, tends to spread out between the WC grains, pulling them together into aggregates and filling in the porosity space. Evolution of specific surface area in Fig.6a shows indeed that the binder phase structure becomes finer up to 1200 °C.

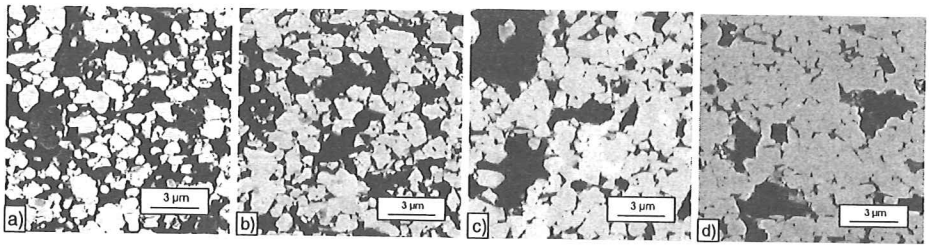

Fig.5. SEM images of the microstructures at different temperatures: a) 1000 °C b) 1100 °C c) 1200 °C d) 1250 °C.

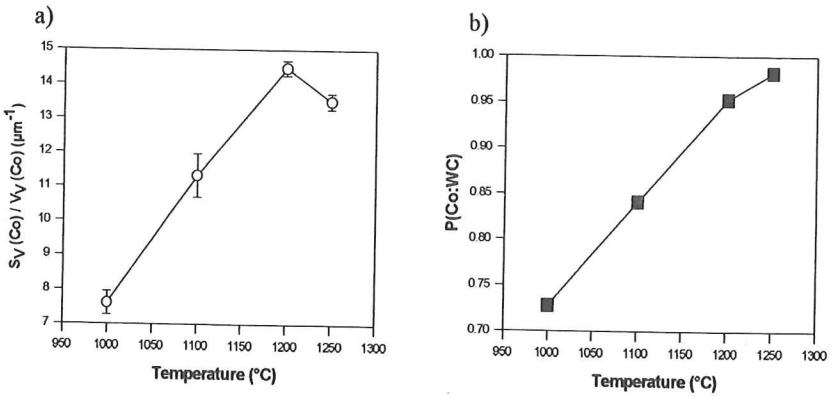

Fig.6. Evolution of the stereological parameters Sv/Vv and P(Co:WC) with the sintering temperature for the cobalt phase.

The probability of contact between the binder and the refractory phases has been defined as:

$$P(Co:WC) = \frac{S_V(Co:WC)}{S_V(Co)}$$

where Sv(Co:WC) is the specific contact area between the cobalt and the WC phases. It continually increases with T_S and reaches 0.97 at 1250 °C as presented in Fig.6b, showing that cobalt wets the WC particles and spreads between them. Cobalt granulometry distribution in Fig.7a confirms that there is a redistribution of solid cobalt when the sintering temperature increases, by which large particles (1-4 μm) disappear to spread between the WC grains.

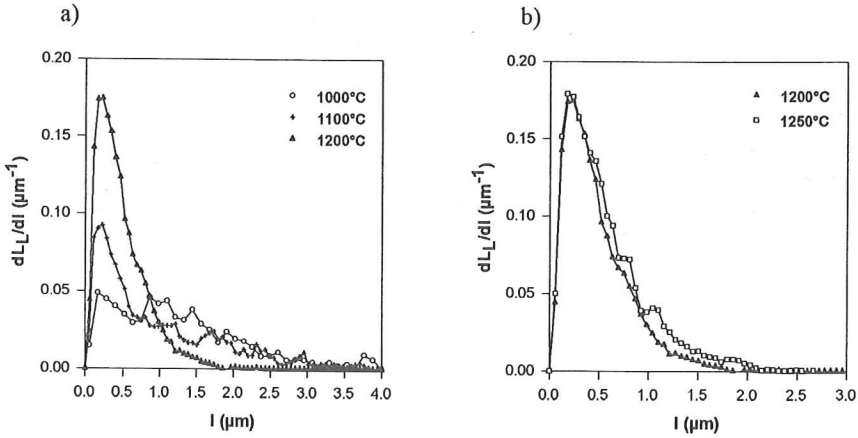

Fig.7. Granulometry of cobalt (length-weighted) as a function of the sintering temperature: a) up to 1200 °C b) above 1200 °C.

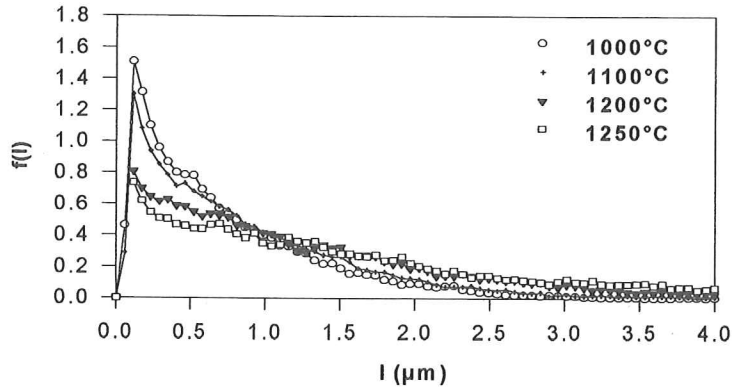

Fig.8. Granulometry of WC as a function of the sintering temperature.

Therefore, it can be asserted that a good wetting of WC by solid cobalt allows the rearrangement of WC grains which brings them closer under capillary forces. Above 1200 °C, both Fig.6a and Fig.7b indicate that cobalt structure slightly coarsens. This might be the result of a secondary rearrangement process induced by the faceting of WC grains which would connect cobalt areas previously separated by WC grains or remaining porosity.

Refractory phase

It can be observed on Fig.5 that submicronic particles, initially present, disappear above 1100°C meanwhile the coarser grains tend to become faceted. No thorough image analysis investigation such as segmentation of WC grains was performed for this phase during this study. However, the carbide granulometric distributions (Fig.8) can be explained by an elimination of submicronic grains above 1100 °C. According to thermodynamic data (Rautala and Norton, 1952), solubility of carbide into the cobalt phase becomes significant around 1100°C which allows one to conclude that small grains are dissolved in the binder phase. It also accounts for the observed faceting of WC grains previously mentioned.

CONCLUSION

SEM-based image analysis has been a very useful technique to follow the microstructural evolution of cemented carbide compacts during solid state sintering. Analysis of chord length distributions and evolutions of stereological parameters like the specific surface area of each phase or the specific contact area between the refractory and the binder phases allows one to characterize the densification in the solid phase; it can be established that, as in liquid-phase sintering, the following mechanisms take place: spreading of cobalt and rearrangement of WC grains under capillary forces, dissolution-precipitation of WC in the cobalt phase leading to shape accomodation processes and secondary rearrangement of WC particles.

ACKNOWLEDGEMENTS

The authors wish to thank the Centre Européen de Recherche en Métallurgie des Poudres (CERMeP) and Sandvik Hard Materials for the suppliance of materials and their financial aid.

REFERENCES

Åkesson L. A sintering study in the WC-Co system. Jernkontorets forskning 1978; 815-74.

Haglund S., Uhrenius B., Ågren J. Solid state sintering of WC-Co. Proceedings of Powder Metallurgy World Congress PM'94 1994; 2: 1493-96.

Kingery W.D. Densification during sintering in the presence of a liquid phase. J. Appl. Phys. 1959; 30: 301-6.

Otsu N. A threshold selection method from gray level histograms. IEEE Trans. Syst. Man.Cybern. SMC 1979; 9: 62-66.

Rautala P., Norton T. Tungsten-Cobalt-Carbon system. Trans. AIME 1952; 1045-50.

Presented at the 9th International Congress for Stereology, Copenhagen, August 20th to 25th, 1995.